Carcinogenesis, 2016, Vol. 37, No. 7, 712–722

doi:10.1093/carcin/bgw050
Advance Access publication April 27, 2016
Original Manuscript

ORIGINAL MANUSCRIPT

Lipocalin 2 prevents oral cancer metastasis through carbonic anhydrase IX inhibition and is associated with favourable prognosis

Chiao-Wen Lin[1,2], Wei-En Yang[3], Wei-Jiunn Lee[4], Kuo-Tai Hua[5], Feng-Koo Hsieh[6], Michael Hsiao[7], Chia-Cheng Chen[8], Jyh-Ming Chow[9], Mu-Kuan Chen[3,10], Shun-Fa Yang[3,11] and Ming-Hsien Chien[4,12,*]

[1]Institute of Oral Sciences, Chung Shan Medical University, Taichung 40201, Taiwan,
[2]Department of Dentistry, Chung Shan Medical University Hospital, Taichung 40201, Taiwan,
[3]Institute of Medicine, Chung Shan Medical University, Taichung 40201, Taiwan,
[4]Department of Medical Research, Wan Fang Hospital, Taipei Medical University, Taipei 116, Taiwan,
[5]Graduate Institute of Toxicology, College of Medicine, National Taiwan University, Taipei 10051, Taiwan,
[6]Experimental Surgery and Regenerative Medicine, Department of Surgery, Ludwig-Maximilians University, 80539 Munich, Germany,
[7]The Genomics Research Center, Academia Sinica, Taipei 115, Taiwan,
[8]Division of Oral and Maxillofacial Surgery, Department of Dentistry, Shin-Kong Memorial Hospital, Taipei 111, Taiwan,
[9]Department of Internal Medicine, Wan Fang Hospital, Taipei Medical University, Taipei 116, Taiwan,
[10]Department of Otorhinolaryngology-Head and Neck Surgery, Changhua Christian Hospital, Changhua 505, Taiwan,
[11]Department of Medical Research, Chung Shan Medical University Hospital, Taichung 40201, Taiwan and
[12]Graduate Institute of Clinical Medicine, Taipei Medical University, Taipei 110, Taiwan

*To whom correspondence should be addressed. Tel: +886 2 27361661; Fax: +886 2 27390500; Email: mhchien1976@gmail.com
Correspondence may also be addressed to Shun-Fa Yang. Tel: +886 4 2473959; Fax: +886-4-24723229; Email: ysf@csmu.edu.tw

Abstract

Lipocalin 2 (LCN2), a secreted glycoprotein, is up- or downregulated in different human cancers. At present, the functional role of LCN2 in the progression of oral squamous cell carcinoma (OSCC), which accounts for most head and neck cancers, remains poorly understood, particularly with respect to its involvement in invasion and metastasis. In this study, we observed that LCN2 expression decreased in patients with OSCC and lymph node metastasis compared with that in patients without metastasis. A higher LCN2 expression correlated with the survival of patients with OSCC. Furthermore, LCN2 overexpression in OSCC cells reduced *in vitro* migration and invasion and *in vivo* metastasis, whereas its silencing induced an increase in cell motility. Mechanistically, LCN2 inhibited the cell motility of OSCC cells through hypoxia-inducible factor (HIF)-1α-dependent transcriptional inhibition of the carbonic anhydrase IX (CAIX). CAIX overexpression relieved the migration inhibition imposed by LCN2 overexpression in OSCC cells. Moreover, a microRNA (miR) analysis revealed that LCN2 can suppress CAIX expression and cell migration through miR-4505 induction. Examination of tumour tissues from patients with OSCC and OSCC-transplanted mice revealed an inverse correlation between LCN2 and CAIX expression. Furthermore, patients with $LCN2^{strong}$/$CAIX^{weak}$ revealed the lowest frequency of lymph node metastasis and the longest survival. Our findings suggest that LCN2 suppresses tumour metastasis by targeting the transcriptional and post-transcriptional regulation of CAIX in OSCC cells. LCN2 overexpression may be a novel OSCC treatment strategy and a useful biomarker for predicting OSCC progression.

Received: October 18, 2015; **Revised:** March 16, 2016; **Accepted:** April 12, 2016

Abbreviations

CAIX	carbonic anhydrase IX
HIF	hypoxia-inducible factor
HRE	hypoxia-response element
IHC	immunohistochemical
LCN2	lipocalin 2
miR	microRNA
OSCC	oral squamous cell carcinoma
RT-PCRs	real-time polymerase chain reactions
SCID	severe combined immunodeficient
3′UTR	3′ untranslated region

Introduction

The incidence of oral squamous cell carcinoma (OSCC), the most common malignant tumour of the head and neck, has recently increased (1). The incidence of neck lymph node metastasis in oral cancer varies from 25 to 65% (2), and the 5-year survival rate is 90% for patients without metastasis but <40% for those with metastasis, suggesting that lymph node metastasis is a key prognostic factor (3,4). However, molecular mechanisms underlying lymph node metastasis remain unclear, and understanding the pathophysiology of lymph node metastasis of OSCC is essential for developing diagnosis, prognosis and targeted therapy.

Lipocalin 2 (LCN2), also known as neutrophil gelatinase-associated lipocalin, of the lipocalin superfamily was originally purified from human neutrophils, which are associated with gelatinase (5). LCN2, initially defined as a strong bacteriostatic agent, is active against various gram-negative microorganisms (6). LCN2 has been identified as a stress protein released in various sterile inflammatory conditions, such as obesity-related inflammation in adipose tissue (7) and cancer (8).

LCN2 expression is high in multiple human cancers, including breast, colorectal, pancreatic and ovarian carcinomas (8,9). LCN2 has functional roles in promoting tumorigenesis through enhancing tumour cell proliferation and metastatic potential (10–12). Mechanistic studies have reported that the major causes of LCN2 for regulating tumour development are a combined expression of LCN2 and MMP-9 for sustaining a high gelatinolytic action of MMP-9 and for promoting epithelial to mesenchymal transition (EMT) (12–15). In contrast to its pro-oncogenic functions, LCN2 suppresses the invasive ability of ovarian and liver cancers by negatively modulating the EMT process (16). Microarray data sets revealed that LCN2 expression in metastatic tissues were significantly lower than that observed in primary tumours of several tumour types (8). Altogether, the aforementioned data indicate that LCN2 plays crucial roles in tumour development and may have pro- or antioncogenic functions.

OSCC accounts for approximately 90% of all head and neck cancers (17). In contrary to most solid tumours, microarray analyses have revealed a lower LCN2 expression in head and neck cancers compared to normal tissues (8). However, the biological roles of low LCN2 expression in head and neck cancers remain unclear. In the present study, we retrospectively analysed LCN2 expression in OSCC specimens and revealed its correlation with survival. We mechanistically examined how LCN2 affects OSCC migration, invasion and metastasis. Our data demonstrate LCN2 to be an OSCC suppressor through downregulating the carbonic anhydrase IX (CAIX) expression via HIF-1α suppression and the miR-4505 induction signalling pathway.

Materials and methods

Patients and specimens

We enrolled 266 patients diagnosed with OSCC at Changhua Christian Hospital (Changhua, Taiwan) between 2000 and 2006, as described in our previous study (18). The study was approved by the Institutional Review Board of Changhua Christian Hospital (CCH No: 101222), and informed written consent was obtained from all patients.

Immunohistochemistry

OSCC tissue microarray block slides were deparaffinised, as stated in our previous study (19). The slides were incubated with 1:50 diluted anti-LCN2 or anti-CAIX antibody (Santa Cruz Biotechnology, Santa Cruz, CA) for 60 min at room temperature. After thoroughly washing with PBS, the conventional streptavidin–biotin peroxidase method (LSAB Kit K675; Dako, Copenhagen, Denmark) using 3,3′-diaminobenzidine (DAB) was employed for assessing signal development. Two pathologists blinded to the clinical outcomes semiquantitatively assessed LCN2 or CAIX expression based on the staining intensity; they independently scored sections through light microscopy. Scores of 0, 1, 2 and 3 indicated negative, weak, moderate and strong staining intensities, respectively.

Materials

Cell culture materials and fetal bovine serum (FBS) were obtained from Gibco-BRL (Gaithersburg, MD). An enhanced chemiluminescence kit was purchased from Amersham (Arlington Heights, IL); anti-β-actin was obtained from BD Biosciences (San Jose, CA). Anti-CAIX and anti-HIF-1α antibodies were purchased from Cell Signaling Technology (Beverly, MA). Anti-LCN2 antibody was purchased from R&D Systems, Inc. (Minneapolis, MN). Unless otherwise specified, all other chemicals used in this study were purchased from Sigma Chemical Co. (St. Louis, MO).

Cell culture

The tumorigenic TW2.6 cells were obtained from Dr Kuo's group where the cell line is originally established and authenticated (20). SAS and HSC-3 cells were purchased from and validated by the Japanese Collection of Research Bioresources Cell Bank (JCRB, Shinjuku, Japan). These cells were all maintained in Dulbecco's Modified Eagle Medium/Nutrient Mixture F-12 (DMEM/F12; Life Technologies, Grand Island, NY) supplemented with 10% FBS (Gibco, Grand Island, NY). SCC9 cells were purchased from and validated by the American Type Culture Collection (ATCC, Manassas, VA) and maintained in DMEM/F12 supplemented with 10% FBS, 400 ng/ml hydrocortisone and 0.1 mM non-essential amino acids (NEAA; Life Technologies). CA9-22 (purchased from and validated by ATCC) and CAL-27 (purchased from and validated by JCRB) cells were maintained in DMEM (Gibco) supplemented with 10% FBS. OECM-1 cells were obtained from Dr Meng's group where the cell line is originally established and authenticated (21) and maintained in RPMI (Gibco) supplemented with 10% FBS. SCC-25 cells (purchased from and validated by ATCC) were maintained in F-12 Medium supplemented with 10% FBS, 400 ng/ml hydrocortisone and 0.5 mM sodium pyruvate. All the cells were cultured and maintained at 37 °C in a 5% CO_2 and 95% air atmosphere.

DNA construction, transient transfection and stable cell clone establishment

Human full-length LCN2 cDNA was cloned into the pcDNA3.1 expression vector. After confirmation through DNA sequencing, the pcDNA3.1–LCN2 expression and pcDNA3.1 control vectors were transiently transfected into SCC9 or TW2.6 cells by using Lipofectamine 2000 (Invitrogen, Carlsbad, CA). Furthermore, SCC9 and TW2.6 cells were stably transfected with pcDNA3.1 or pcDNA3.1–LCN2 expression vectors and selected using G418 (250 μg/ml).

In vitro wound closure assay

SCC9 (8×10^5 cells/dish) and TW2.6 (2×10^6 cells/dish) cells were plated in 6 cm dish for 24 h, wounded by scratching with a pipette tip, and incubated with a DMEM/F12 medium containing 0.5% FBS for 0, 12, 24 and 48 h. Cells were imaged through phase-contrast microscopy (100×), as previously described (22).

Cell invasion and migration assays

Cell invasion and migration assays were performed according to the methods described by Yang *et al*. (23). The cells were harvested and seeded in a Boyden chamber (Neuro Probe, Cabin John, MD; 10^4 cells/well) in a serum-free medium and incubated for 24 h. For invasion assay, 10 µl Matrigel (25 mg/50 ml; BD Biosciences, MA) was applied to polycarbonate membranes (pore size, 8 µm), and the bottom chamber contained a standard medium. The invaded cells were stained using 5% Giemsa and enumerated through light microscopy. The migration assay was performed as was the invasion assay but without Matrigel coating.

Western blot analysis

Protein lysates were prepared as previously described (24), and Western blot analysis was performed using specific primary antibodies.

RNA isolation, reverse transcription polymerase chain reaction and microarray

mRNA was isolated and amplified as previously described (24), and primer sequences are shown as supplementary data (Supplementary Table 1, available at *Carcinogenesis* Online). For cDNA or miRNA microarray, RNA isolated from SCC9/Neo or SCC9/LCN2 was submitted to the Phalynx Biotech Group (Hsinchu, Taiwan) for expression profiling and analysis.

TaqMan miRNA real-time reverse transcription polymerase chain reaction

To determine miR-4505 expression in OSCC cells, we used the TaqMan MicroRNA Assay kit (Applied Biosystems, Carlsbad, CA) according to manufacturer instructions. Real-time polymerase chain reactions (RT-PCRs) were conducted in 20 µl of a reaction mixture containing 2 µl of the reverse transcription product, 10 µl of 2× Taqman Universal PCR Master Mix, 7 µl of water and 1 µl of the TaqMan assay probe. The relative miRNA expression was analysed through the Ct method and was normalised to RNU6B expression.

Small interfering RNA transfection

LCN2 gene silencing was performed using siRNAs targeting LCN2 and a negative control (Applied Biosystems). Each siRNA (150 pmol) was transfected into OSCC cells for 48 h by using the Lipofectamine RNAiMAX Transfection reagent (Invitrogen) according to manufacturer instructions.

Construction of the HIF-1α-binding site mutant CA9 promoter/reporter plasmids

All promoter fragments were cloned in the pGL3 basic vector (Promega). The CAIX-Luc promoter sequence contains −173 to 37 fragments, which were isolated through PCR amplification by using Kpn I forward primer (5′-GGTACCACCTGCCCCTCACTCCAC-3′) and Sac I reverse primer (5′-GAGCTCCTGACTGTGGGGTGTCC-3′). HREm-CAIX-Luc was constucted using a QuikChange site-directed mutagenesis kit system (Stratagene) according to manufacturer instructions. The mutated oligonucleotides were constructed using the primer 5′-GTTTCCAATGCT*TT*TACAGCCCGTAC-3′. Both constructs in promoter fragments were sequence-verified.

In vivo spontaneous metastasis model

All animal studies were performed according to protocols approved by the Institutional Animal Care and Use Committee of Taipei Medical University. Age-matched male severe combined immunodeficient (SCID) mice (6–8 weeks old) were used in assays for tumour growth and metastasis in an orthotopic graft model. LCN2-expressing luciferase-tagged TW2.6 cells (5×10^5) or the control vector were suspended in phosphate-buffered saline:Matrigel (1:1) and directly injected into the lips of SCID mice ($n = 6$ per group). After detecting tumour growth, lymph node metastasis was monitored once per week by using a non-invasive bioluminescent imaging system (Xenogen IVIS-200 system). Metastatic neck lymph nodes were enumerated, and the volume was quantified 35 days after cell injection.

Statistical analysis

All experiments were conducted in triplicate. Values are presented as the mean ± standard error (SE). Statistical analysis was performed using Statistical Package for Social Science, Version 16 (SPSS, Chicago, IL). Data were analysed using the Student's *t*-test for comparing two groups. One-way analysis of variance (ANOVA) followed by Tukey's *post hoc* test were used for analysing three or more groups. Clinicopathological data were statistically analysed using chi-squared and Fisher's exact tests. *p* values of < 0.05 were considered statistically significant.

Results

LCN2 expression inversely correlated with the stage and lymph node metastasis and positively correlated with the survival of patients with oral cancer

To examine LCN2 expression in patients with OSCC, 516 head and neck cases were analysed from The Cancer Genome Atlas (TCGA). Significant low LCN2 transcript was observed in tumour as compared with normal tissue (Figure 1A, left panel). An analysis of 45 matched tumour tissues and the corresponding normal tissues revealed lower LCN2 expression in the tumours (Figure 1A, right panel). Immunohistochemical (IHC) staining was performed on a tissue microarray for examining the clinical relevance of LCN2 expression in another OSCC cohort ($n = 266$). All positive cases revealed a diffuse cytoplasmic LCN2 distribution in cancer cells (Figure 1B). Supplementary Table 2, available at *Carcinogenesis* Online, illustrates the association between selected clinicopathological factors and LCN2 expression. When LCN2 expression was classified into a two-tier grading system of weak (−/1+) and strong (2+/3+) LCN2 staining, LCN2 expression inversely correlated with lymph node metastasis and the clinical stage (Supplementary Table 2, available at *Carcinogenesis* Online; Figure 1C). Moreover, we collected 18 sets of individually matched samples from primary tumours and lymph node metastasis; in 11 out of 18 patients, LCN2 expression was significantly lower in lymph node metastatic tumours than in primary OSCC cells (Figure 1D and E, $P = 0.017$). These results indicate the inverse correlation of LCN2 with OSCC, particularly in lymph node metastasis. The Kaplan–Meier plot reveals a favourable overall survival of patients with a strong LCN2 expression ($P = 0.001$; Figure 1F), and the univariate Cox regression analysis revealed that a strong LCN2 expression was a significant predictor of an optimal outcome (Supplementary Table 3, available at *Carcinogenesis* Online).

LCN2 expression suppresses the migratory and invasive abilities of OSCC cells

Our clinical findings suggest that LCN2 plays a role in the invasive and metastatic abilities of OSCC cells. We next evaluated the function of LCN2 in cell migration and invasion, the fundamental steps of tumour metastasis. Relative LCN2 expression in eight human OSCC cell lines was evaluated (Figure 2A). We overexpressed LCN2 and established LCN2-stably transfected SCC9 and TW2.6 cells (Figure 2B and Supplementary Figure 1A, available at *Carcinogenesis* Online). Figure 2C and Supplementary Figure 1B, available at *Carcinogenesis* Online, illustrate the dramatically suppressed wound closure ability of both LCN2-transfected SCC9 and TW2.6 cells. A Boyden chamber assay was further performed for investigating the effects of LCN2 on the migratory and invasive abilities of OSCC cells, which revealed significantly suppressed abilities of both LCN2-transfected SCC9 and TW2.6 cells (Figure 2D; Supplementary Figure 1C, available at *Carcinogenesis* Online). The transfection and expression of LCN2-specific siRNA significantly reduced LCN2 mRNA and protein expression (Figure 2E, upper panel), with concomitantly increasing the migratory and invasive

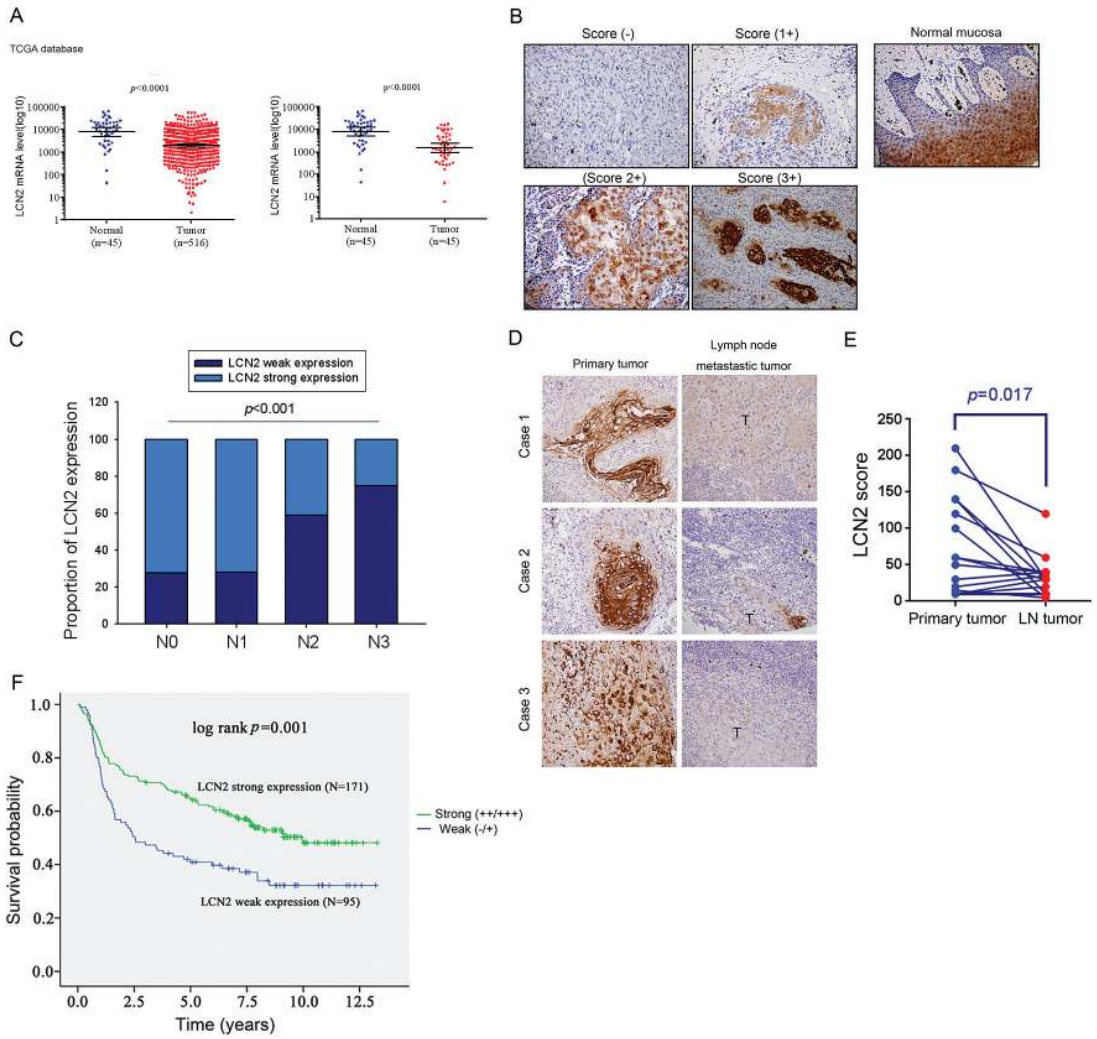

Figure 1. LCN2, expressed by cancer cells, is inversely correlated with the clinical stage and lymph node metastasis and positively correlated with the survival of patients with OSCC. (**A**) LCN2 expression in head and neck cancer specimens (n = 516) or paired cancer samples (n = 45) and normal tissue samples (n = 45) were measured through RNA sequencing obtained from the TCGA. ***P < 0.001. (**B**) Tissue microarrays of primary OSCCs cells (n = 266) were immunohistochemically analysed for LCN2. Representative images of IHC staining revealing weak (– or 1+) and strong (2+ or 3+) LCN2 expression. Histopathological images are shown at 200× magnification. (**C**) Negative correlation between LCN2 expression and lymph node metastasis. Weak LCN2 expression (–/1+) is shown as deep blue columns, whereas strong LCN2 expression (2+/3+) is shown as light blue columns. Results were analysed using the χ^2 test. (**D**) Representative images of IHC staining of LCN2 in matched specimens of primary OSCCs and lymph node metastases. T, tumour cells in lymph node. (**E**) Plot representation of scores according to cytoplasmic IHC expression of LCN2 in primary OSCCs related to the lymph node metastases. The scores are calculated by intensity × percentage of stained cells. (**F**) The Kaplan–Meier plot of overall survival of 266 patients with OSCC stratified by LCN2 expression. A log rank test was used for examining between-group differences.

abilities of LCN2-transfected SCC9 cells compared to control siRNA-transfected cells (Figure 2E, lower panel); this observation confirms that LCN2 modulates the cell motility phenotype. In addition, the rescued phenotypes were observed in TW2.6 cells (Supplementary Figure 1D, available at *Carcinogenesis* Online). Moreover, manipulating LCN2 expression did not significantly affect cell proliferation during the experimental period (Supplementary Figure 2, available at *Carcinogenesis* Online). The cell migratory and invasive abilities of SCC9 cells was attenuated using 500 nM rh LCN2 (Figure 2F). Compared with SCC9 and TW2.6 cells, the higher endogenous LCN2 expression cell lines, CAL-27 and CA9-22 (Figure 2A), were knockdowned of LCN2 by a siRNA and the migratory (Figure 2G, lower panel) and invasive (Figure 2H) abilities significantly increased. The knockdown efficiency of LCN2 siRNA was detected through Western blotting (Figure 2G, upper panel). These results indicate that LCN2 is crucial in OSCC cell motility.

LCN2-induced suppression of tumour growth and lymph node metastasis in an orthotopic graft model

We examined the *in vivo* effects of LCN2 expression on tumour growth and metastasis. Luciferase-expressing TW2.6-Luc cells were established, and tumour growth and metastasis were monitored through bioluminescence imaging. Control TW2.6 cells (Tw2.6/Neo-Luc) orthotopically injected into SCID mice revealed larger tumours than did Tw2.6/LCN2-Luc cells injected in the mice after 32 days, as revealed by photon emission detection (Figure 3A). Body weights of the TW2.6/Neo- and TW2.6/LCN2-injected mice did not differ significantly (Figure 3C). Mice were killed at the end of the experiment, and *ex vivo* images of their neck lymph nodes revealed a lower intensity in TW2.6/LCN2-Luc-injected mice than in TW2.6/Neo-Luc-injected mice (Figure 3B). Most mice developed neck lymph node metastasis within 32 days after cancer cell injection; we further determined the frequency of neck

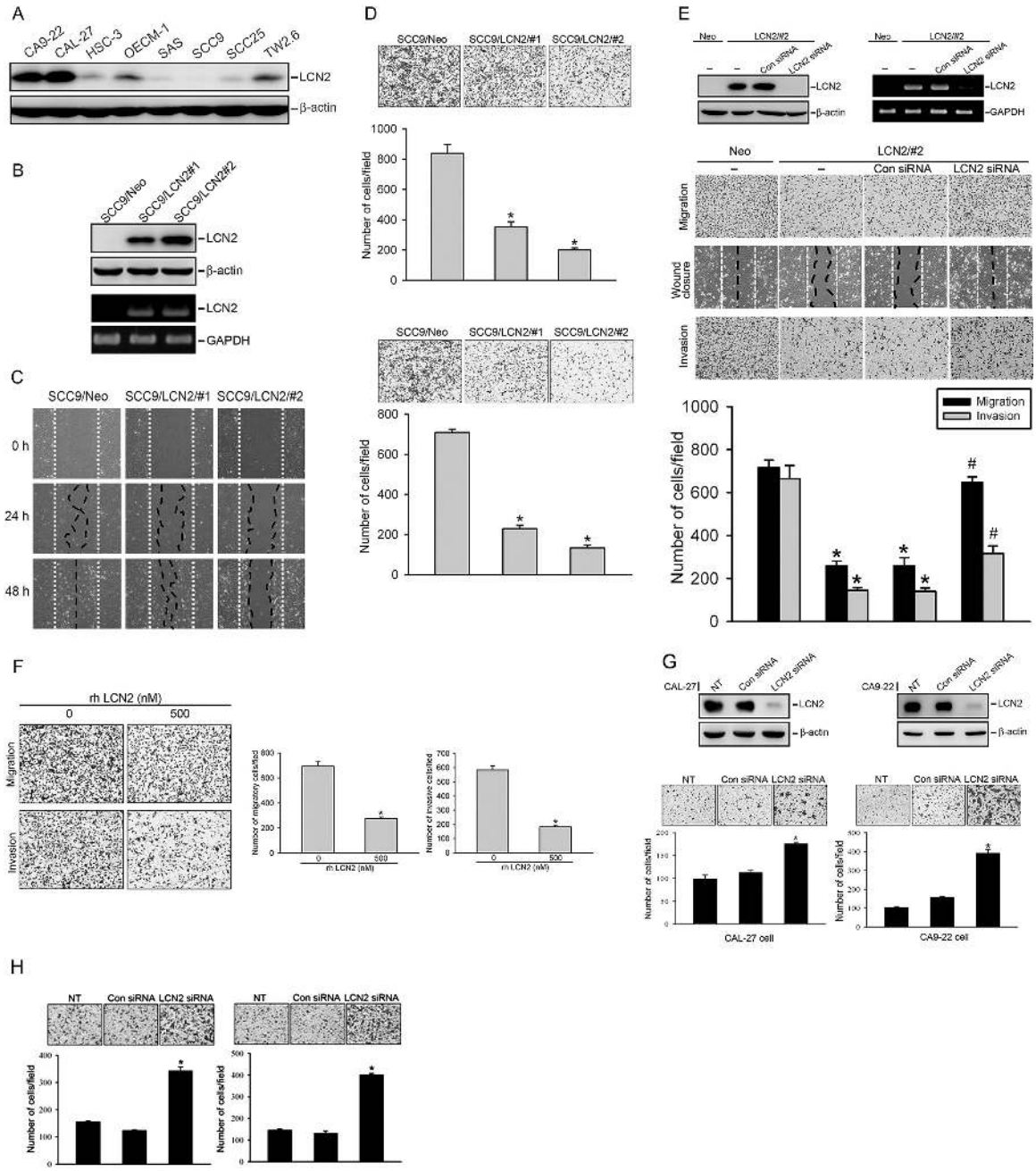

Figure 2. LCN2 regulates the migratory and invasive abilities of OSCCs. (**A**) Endogenous LCN2 protein levels were detected using Western blot analysis in human OSCC cells. (**B**) SCC9 cells expressing low LCN2 were transiently transfected with a vector control (pcDNA 3.1) or LCN2-expressed vector (pcDNA-LCN2) for generating stably transfected clones (SCC9/Neo and SCC9/LCN2) after G418 (250 μg/ml) selection. LCN2 protein and mRNA levels in LCN2-stably transfected SCC9 cells were detected through Western blotting (upper panel) and RT-PCR (lower panel), respectively. (**C**) Migratory abilities of SCC9/Neo and SCC9/LCN2 cells were evaluated using the wound healing assay. Furthermore, cells were wounded, observed for 24 and 48 h thereafter, and analysed through phase-contrast microscopy. (**D**) The migratory and invasive abilities of SCC9/Neo and SCC9/LCN2 cells were evaluated using Boyden chamber migration (upper panel) and Matrigel invasion (lower panel) assays. Differences are presented as the mean of triplicate experiments compared with control cells. *$P < 0.05$ compared with control cells. (**E**) Upper panel, SCC9/LCN2 cells were transiently transfected with control or LCN2 siRNA. The knockdown efficiency was evaluated through Western blotting and RT-PCR. Lower panel, migratory and invasive abilities of SCC9/Neo and SCC9/LCN2 cells expressing control or LCN2 siRNA were evaluated through wound healing, Boyden chamber migration and Matrigel invasion assays. Differences are presented as the mean of triplicate experiments compared with control cells. *$P < 0.05$ compared with SCC9/Neo cells. #$P < 0.05$ compared with control siRNA-transfected SCC9/LCN2 cells. (**F**) SCC9 cells were treated with vehicle or 500 nM LCN2 for 24 h. Cell mobility was evaluated using the Boyden chamber assay, and representative images of individual groups are shown; the migration and invasion of SCC9 cells were quantified, and data are presented from three independent experiments. *$P < 0.05$ compared with vehicle groups. (**G**) Upper panel, CAL-27 and CA9-22 cells highly expressing LCN2 were transiently transfected with control or LCN2 siRNA. The knockdown efficiency was evaluated through Western blotting. Lower panel, migratory abilities of CAL-27 (left) and CA9-22 (right) cells expressing control or LCN2 siRNA. (H) Invasive abilities of CAL-27 (left) and CA9-22 (right) cells expressing control or LCN2 siRNA. Differences are presented as the mean ± SE from three independent experiments. *$P < 0.05$ compared with control cells.

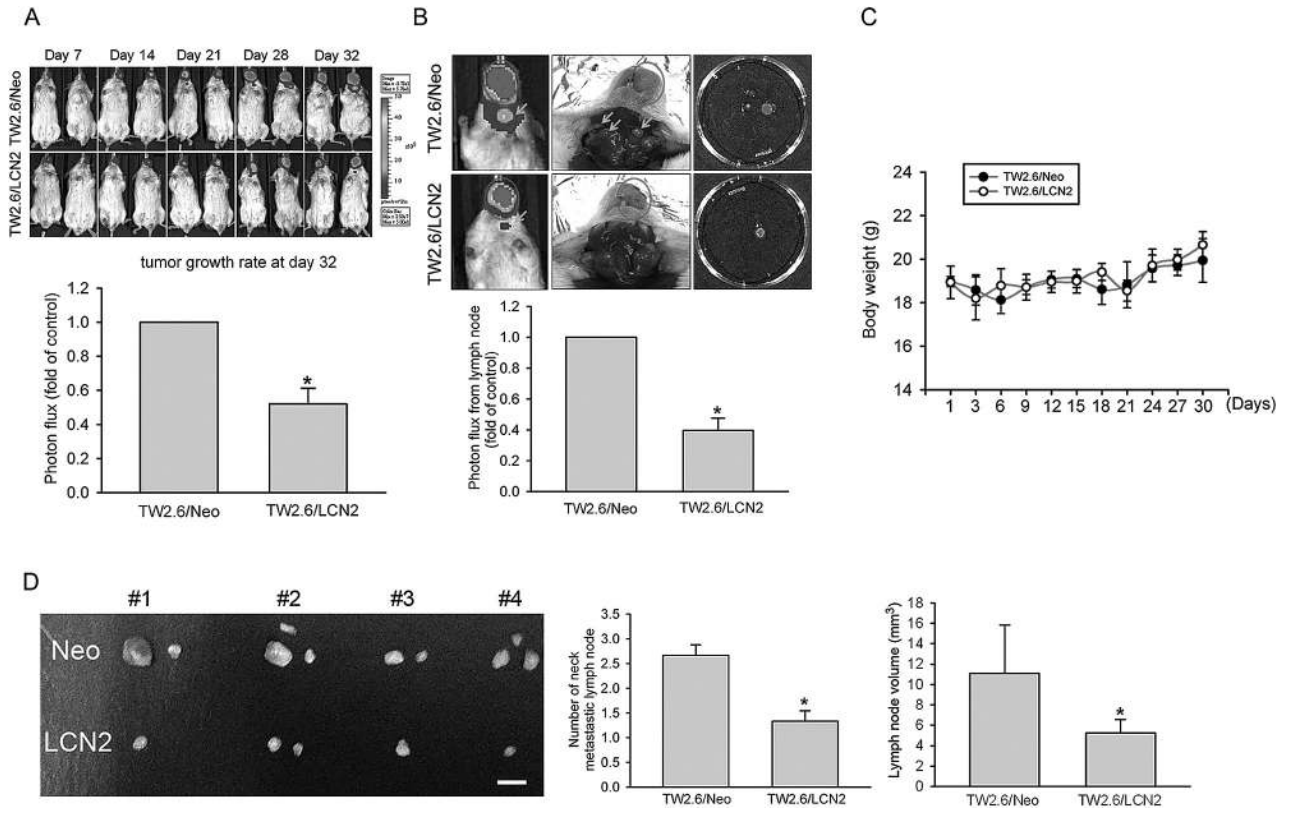

Figure 3. LCN2 suppresses tumour growth and lymph node metastasis in a TW2.6 orthotopic graft model. **(A)** Luciferase-tagged TW2.6/Neo or TW2.6/LCN2 cells were orthotopically injected into mice. Upper panel represents the luciferase activity image. After 32 days of tumour cell injection, tumours from six mice injected with TW2.6/Neo or TW2.6/LCN2 were quantified by measuring the photon influx (lower panel). A significant difference was observed between the groups (*$P < 0.05$) **(B)** Lymph node metastasis was bioluminescently imaged at the end of the study (upper panel) with the mean signal for each group indicated ($n = 6$; lower panel). *$P < 0.05$ compared with the vehicle groups. Red circles in the upper panel indicate primary tumour, and blue arrows indicate lymph node metastasis. **(C)** Changes in body weight (g) during the experiment. **(D)** Macroscopic analysis of neck lymph nodes. The appearance, number and volume of neck lymph nodes were photographed, enumerated and measured after removal. The metastatic lymph node number and volume were significantly lower in TW2.6/LCN2 mice than in TW2.6/Neo mice, as indicated by asterisks (*$P < 0.05$). Scale bar = 0.5 cm.

lymph node metastasis and volume of lymph node excised from the TW2.6/Neo and TW2.6/LCN2 groups. The mean numbers and volume of neck metastatic lymph nodes in TW2.6/LCN2 mice significantly decreased compared with those in TW2.6/Neo mice (Figure 3D). To rule out the possibility that the antimetastastic effect of LCN2 in the orthotopic metastatic mouse model was because of the LCN2-mediated growth inhibition of primary tumour, we investigated the antimetastatic effect of LCN2 in the experimental metastasis model by using the bioluminescence system. TW2.6 cells (Neo or LCN2 overexpression) were injected into the lateral tail vein of NOD/SCID/IL2rγ^{null} (NSG) mice. Five weeks postinjection, TW2.6 cells overexpressing LCN2 exhibited lower lung colony formation, suggesting that LCN2 overexpression effectively inhibited the metastasis of OSCC tumours in vivo (Supplementary Figure 3, available at Carcinogenesis Online).

cDNA microarray analysis of gene expression profiles reveal an association between LCN2 and HIF-1α-mediated CAIX signalling

To explore the downstream route of LCN2, we compared cDNA microarray analysis results of gene expression profiles of SCC9/LCN2 and SCC9/Neo cells (Figure 4A) and observed that *CA9* and *HIF-1A* are the most significantly downregulated genes in LCN2-overexpressed cells (Figure 4A). Western blotting and RT-PCR revealed that HIF-1α and CAIX protein and mRNA expression were significantly attenuated in the LCN2-overexpressed SCC9 and TW2.6 OSCC cells compared with those in their parental cells (Figure 4B). CAIX protein expression was also inhibited in SCC9 and TW2.6 cells transiently transfected with LCN2 (Supplementary Figure 4, available at *Carcinogenesis* Online). The promoter activity of *CA9* was significantly lower in SCC9/LCN2 cells than in parental SCC9 cells (Figure 4C), indicating that LCN2 regulates CAIX expression, at least partially, at the transcriptional level. HIF-1α has been reported to regulate *CA9* gene expression by binding on hypoxia-response element (HRE) within the basal promoter of *CA9* (25). To determine if HIF-1α participates in LCN2-modulated *CA9* transcription, we generated a promoter with a mutated HRE, with which HIF-1α cannot bind. Results revealed that the inhibitory potential of LCN2 against the *CA9* promoter activity was significantly reversed by the mutated HRE (Figure 4D). These results further indicate that the HIF-1α transcription factor and HRE in the *CA9* promoter region contribute, at least in part, to the LCN2-induced inhibition of *CA9* transcription. CAIX has been reported to correlate with lymph node metastasis of OSCC patients (26). CAIX overexpression significantly increased the CAIX protein levels (Figure 4E, left panel) and reversed the LCN2-mediated inhibition of the migratory ability of SCC9 cells (Figure 4E, right panel), suggesting that HIF-1α-mediated CAIX expression is involved in LCN2-mediated cell motility.

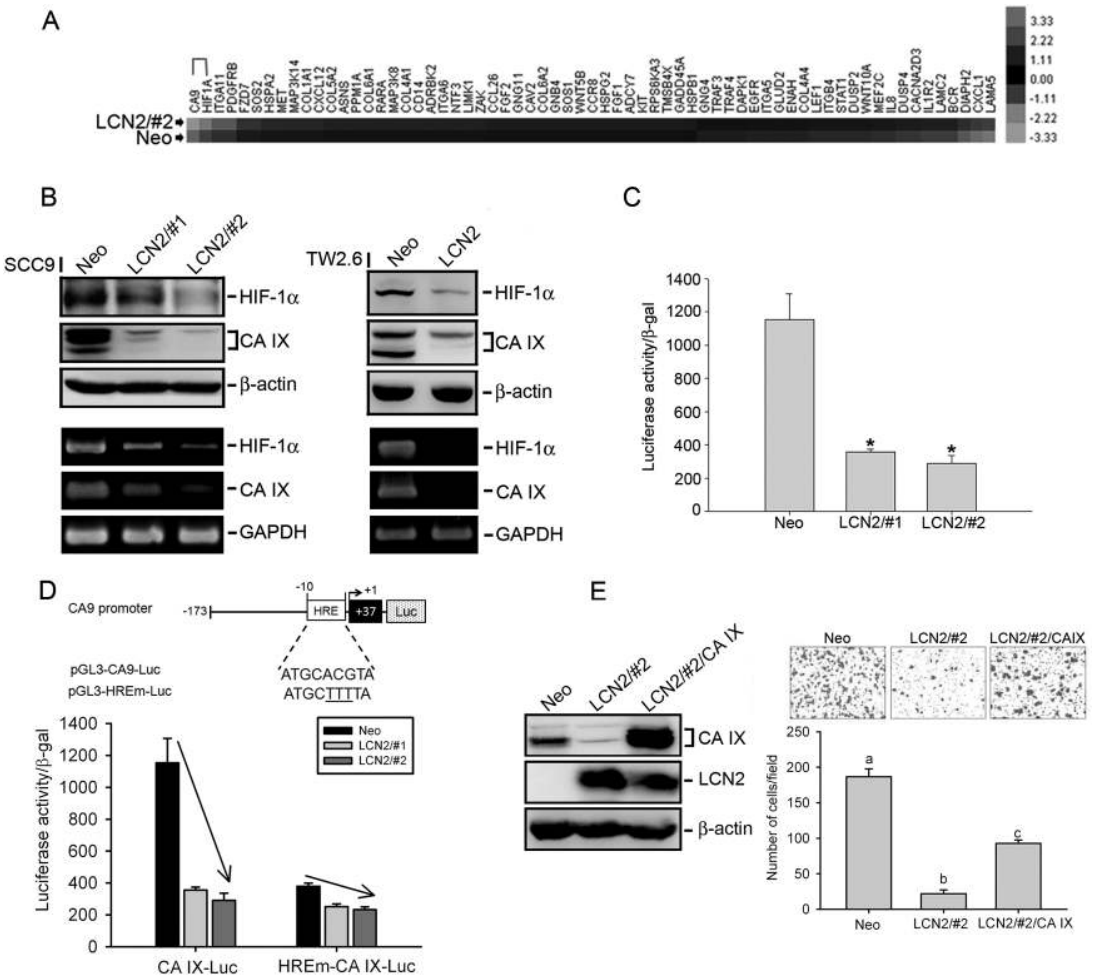

Figure 4. HIF-1α-CAIX signalling is involved in LCN-2-mediated mobility of OSCCs. (**A**) Summary of cDNA microarray analyses. Forty-one genes expressed at least two-fold lower expression of LCN2 in SCC9 cells than in control cells, as assessed using Affymetrix microarray analyses. *CA9* and *HIF1A* are the top two downregulated genes in LCN2-overexpressing cells. (**B**) Western blotting and RT-PCR for reconfirming the expression profile of the HIF-1α and CAIX in LCN2-overexpressing SCC9 (left panel) and TW2.6 (right panel) cells. β-Actin and GAPDH were used as the internal controls. (**C**) A *CA9* promoter reporter assay was conducted for analysing the promoter activity of *CA9* in LCN2-overexpressing or control cells. (**D**) Upper panel, schema of the promoter region of human *CA9* and the used wild-type and mutant constructs. Lower panel, SCC9/LCN2 or SCC9/Neo cells were co-transfected with *CA9* promoter constructs (wild-type or HRE-mut) and the pSV-β-galactosidase control vector. Luciferase activity from (**C**) and (**D**), determined in triplicates, was normalised to the β-galactosidase activity. Differences are presented as the mean of triplicate experiments compared with control cells. *$P < 0.05$ compared with control cells. (**E**) Right panel, migration of SCC9/LCN2 or SCC9/Neo cells transfected with either control vector or pcDNA3.0-CAIX was determined through the Boyden chamber migration assay. SCC9 cell migration was assessed, and data are presented as the mean ± SE of three independent experiments. Data were analysed using a one-way ANOVA with Tukey's *post hoc* tests at 95% confidence intervals; different letters represent different significance levels. Left panel, Western blotting of LCN2 and CAIX protein expressions in SCC9 cells transfected with control vector, LCN2 and LCN2 + CAIX.

Upregulated miR-4505 is involved in the LCN2-mediated suppression of CAIX expression and cell motility

miRNA is a major regulator of cancer progression and metastasis, including that of OSCC (27). In addition to determining the LCN2-induced transcriptional regulation of CAIX, we investigated whether miRNA participates in the LCN2-mediated suppression of CAIX and cell motility. To identify LCN2-regulated miRNAs, a high throughput and specific miRNA microarray (human miRNA OneArray® miRNA profiling chip) by using SCC9/Neo and SCC9/LCN2 cells was conducted by the Phalanx Biotech Group (Hsinchu, Taiwan). miRNA expression upregulated or downregulated by LCN2 overexpression were depicted as a heat map, and the upregulated miRNAs were further analysed using the miRNA target database, TargetScan, for identifying miR-4505 that might target CAIX (Figure 5A). To further confirm expressions of this miRNA, we performed a TaqMan quantitative RT-PCR and observed that miR-4505 expression was significantly upregulated in SCC9 and TW2.6 cells stably transfected with LCN2 compared with that in parental cells (Figure 5B; Supplementary Figure 5A, available at *Carcinogenesis* Online). Moreover, the endogenous CAIX expression in SCC9 or TW2.6 cells was downregulated after transfection with a miR-4505 mimic (Figure 5C; Supplementary Figure 5B, available at *Carcinogenesis* Online). Next, to examine whether miR-4505 regulates the 3′ untranslated region (3′UTR) of *CA9*, we used a luciferase reporter vector harbouring the 3′UTR of *CA9* and transfected this vector combined with the miR-4505 mimic or a mimic control into SCC9 cells. The results revealed that the miR-4505 mimic reduced the luciferase activity compared with that in negative control-transfected cells (Figure 5D). These data demonstrated that miR-4505 can be regulated by LCN2 in SCC9 cells and directly represses CAIX protein expression through binding to the 3′UTR of the *CA9* gene. To verify the direct effect of miR-4505 on cell motility, we transiently overexpressed

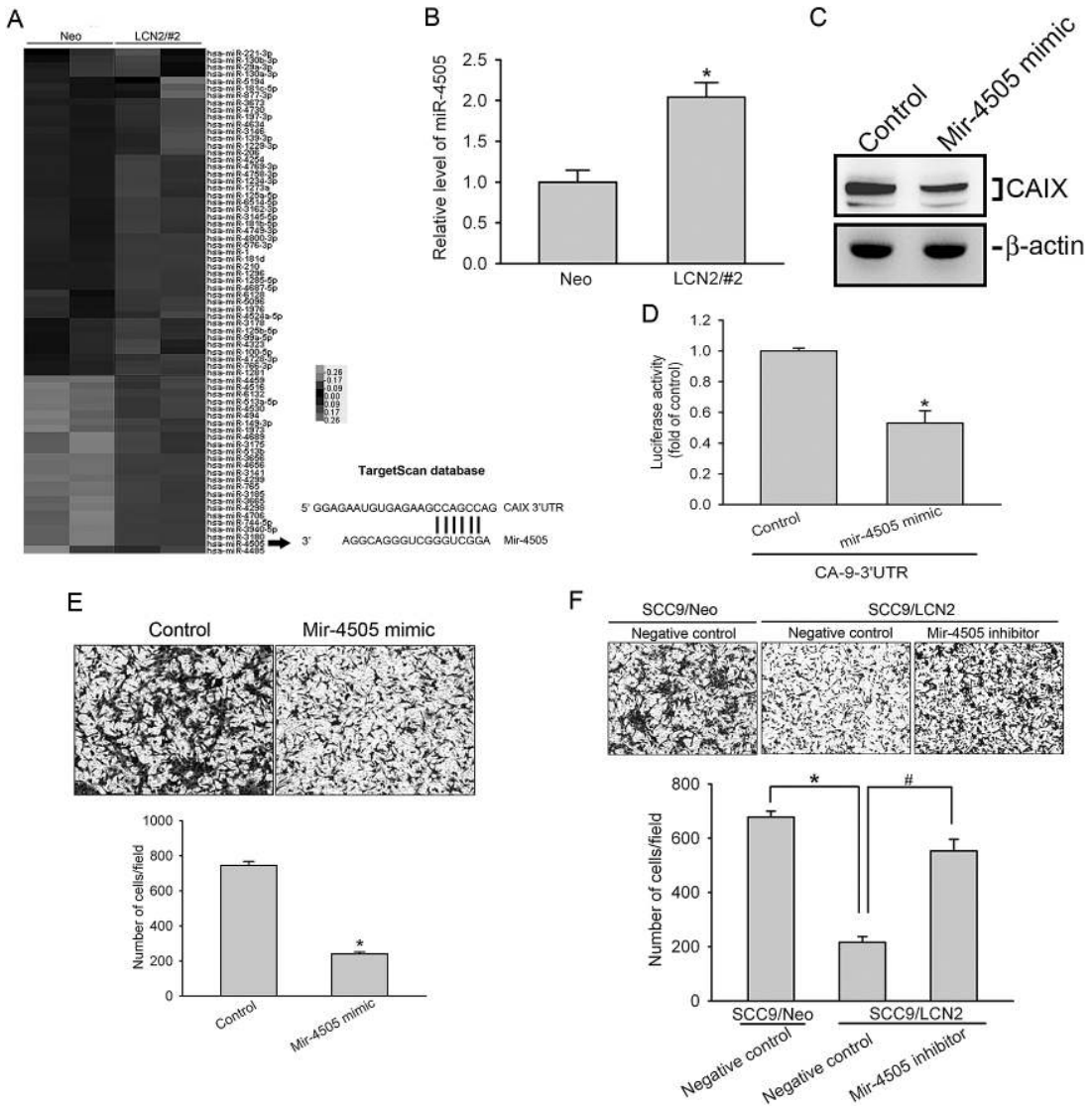

Figure 5. Upregulated miR-4505 is involved in the LCN2-mediated suppression of CAIX expression and cell motility. (**A**) A schema of miRNA selection procedure. Differential expressions of miRNAs in LCN2-overexpressing cells versus control cells were analysed using a OneArray® miRNA profiling chip. (**B**) Quantitative PCR was used for detecting miR-4505 expression in SCC9/Neo and SCC9/LCN2 cells. Values are presented as the mean ± SE of three independent experiments. *P < 0.05 compared with the control groups. (**C**) SCC9 cells were transfected with an miR-4505 mimic or mimic control for 72 h, and CAIX expression was determined using a Western blot analysis. The CAIX protein level was adjusted to the β-actin protein level. (**D**) Relative luciferase activities of SCC9 cells co-transfected with a CA9 luciferase 3′UTR reporter vector and miR-4505 mimic or mimic control for 24 h. Values are presented as the mean ± SE of three independent experiments. *P < 0.05 compared with the control groups. (**E, F**) SCC9/Neo and SCC9/LCN2 cells were respectively transfected with miR-4505 mimic (E) and miR-4505 inhibitor (F) or their respective controls for 72 h. The cell migratory ability was determined using a Boyden chamber migration assay. Values are presented as the mean ± SE of three independent experiments. *P < 0.05 compared with the control groups. #P < 0.05 compared with negative control-transfected SCC9/LCN2 cells.

miR-4505 into SCC9/Neo or TW2.6/Neo cells, in which the migratory ability was significantly downregulated compared with that in control cells (Figure 5E; Supplementary Figure 5C, available at *Carcinogenesis* Online). Moreover, the overexpression of the miR-4505 inhibitor or antagomiR-4505 into SCC9/LCN2 cells reversed the LCN2-mediated inhibition of the migratory ability (Figure 5F; Supplementary Figure 5D, available at *Carcinogenesis* Online). Our results indicate that LCN2 suppresses OSCC motility through miR-4505-mediated CAIX suppression.

Lymph node metastasis ratio is low in patients with OSCC patients having LCN2^{strong}/CAIX^{weak}

To examine the association between LCN2 and CAIX expression in OSCC, we performed IHC analysis of LCN2 and CAIX on primary tumour tissues from 266 patients with OSCC. Patients with a high LCN2 expression and low CAIX (LCN2^{strong}/CAIX^{weak}) expression were more non-predisposed to advanced disease and lymph node metastasis than those having tumours expressing LCN2^{weak}/CAIX^{strong}, LCN2^{weak}/CAIX^{weak} and LCN2^{strong}/CAIX^{strong} (Figure 6A). The association between LCN2 and CAIX expression and the clinicopathological characteristics of OSCC are summarised in Supplementary Table 4, available at *Carcinogenesis* Online. Most importantly, patients having tumours with LCN2^{strong}/CAIX^{weak} had the longest survival time compared to LCN2^{weak}/CAIX^{strong}, LCN2^{weak}/CAIX^{weak} or LCN2^{strong}/CAIX^{strong} groups (Figure 6B). The representative IHC staining patterns of LCN2^{strong}/CAIX^{weak} and LCN2^{weak}/CAIX^{strong} from consecutive serial sections of OSCC are shown in Figure 6C. Moreover, we detected CAIX protein expression of xenografts harvested from TW2.6/Neo- or TW2.6/LCN2-injected

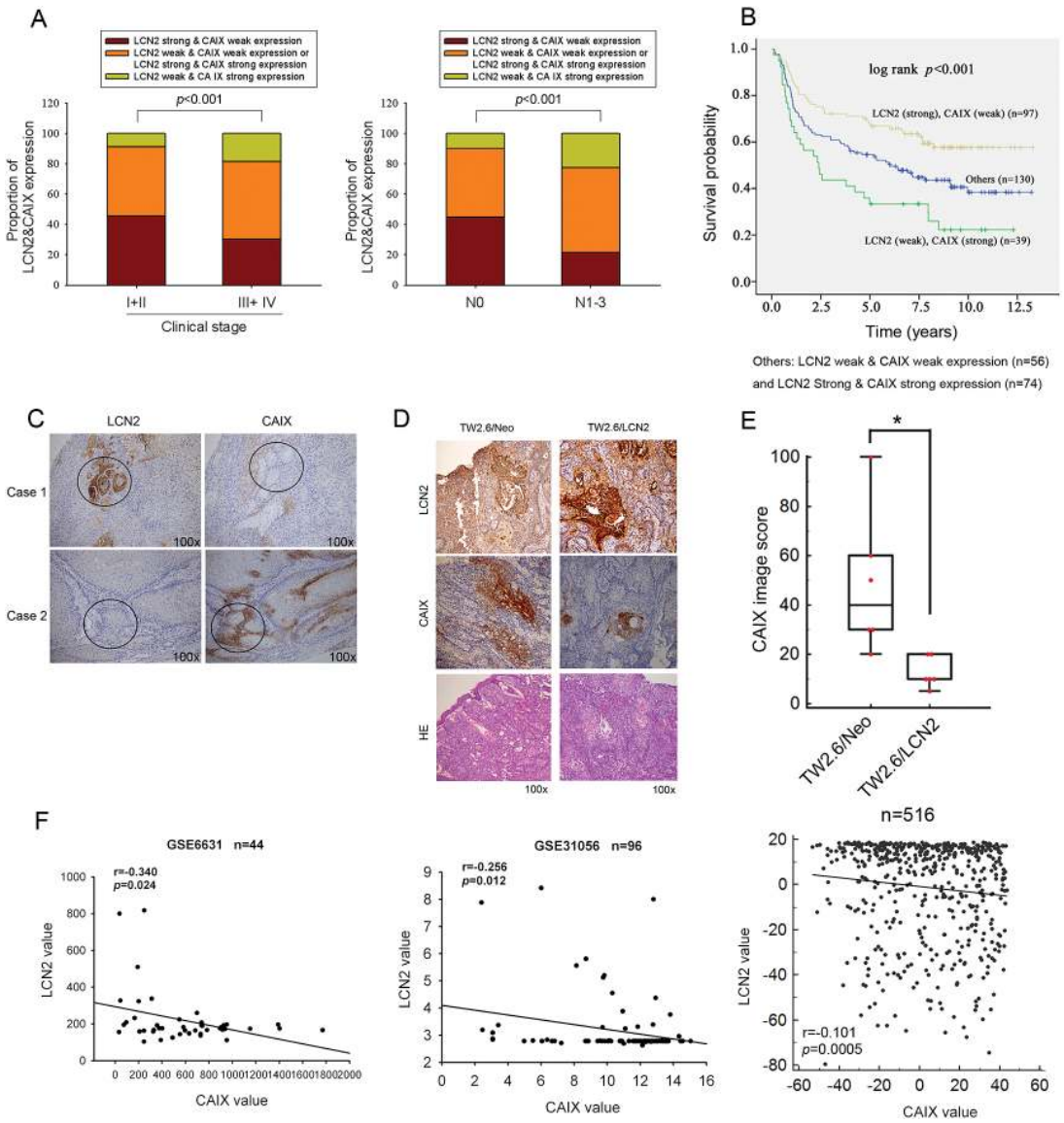

Figure 6. Lymph node metastasis ratio is low in OSCC patients with LCN2^{strong}/CAIX^{weak}. (**A**) Association of combined expression of LCN2 and CAIX with the clinical stage (I–IV) or lymph node metastasis (N0–N3) in patients with OSCC. Results were analysed using the χ^2 test. (**B**) Kaplan–Meier curves for overall OSCC patient survival, grouped by LCN2 and CAIX expression. *P* value refers to the comparison among LCN2^{strong}/CAIX^{weak}, LCN2^{weak}/CAIX^{strong} and others groups, as indicated. (**C**) IHC analysis of serial sections of OSCC specimens from representative patients with OSCC reveals the inverse expression of LCN2 and CAIX on identical localization (black circle indicated). Original magnification, ×100. (**D**) Representative images of IHC staining showing a negative correlation between LCN2 and CAIX in TW2.6 xenografts harvested from TW2.6/Neo- or TW2.6/LCN2-injected mice. Original magnification, ×100. (**E**) Plot representation of scores according to the IHC expression of CAIX in TW2.6/Neo xenografts ($n = 6$) associated with TW2.6/LCN2 xenografts ($n = 6$). The scores are calculated as intensity × percentage of stained cells. (**F**) The association between LCN2 and CAIX in head and neck cancer specimens from GEO (GSE6631 and GSE31066) and TCGA: Spearman's non-parametric correlation test showing a negative correlation between LCN2 and CAIX in head and neck cancers. $\rho = -0.34$, $P = 0.024$; $\rho = -0.26$, $P = 0.012$; $\rho = -0.1$, $P = 0.0005$.

mice and observed that CAIX expression significantly decreased in tumours isolated from TW2.6/LCN2-injected mice (Figure 6D and E). Furthermore, we analysed the correlation between *LCN2* and *CA9* expression using gene expression data obtained from the publicly available Gene Expression Omnibus database (GSE6631 and GSE31056) and the TCGA revealed that LCN2 expression in head and neck cancers tended to inversely correlate with *CA9* (Figure 6F).

Discussion

Despite significant advances in the diagnosis and treatment of patients with cancer, tumour metastasis remains the leading cause of morbidity and mortality. Lymph node metastasis is the major factor for poor prognosis in OSCC (28). However, the factors for OSCC metastasis remain elusive. Our findings reveal that LCN2 expression is inversely correlated with lymph node metastasis and the survival rate and that LCN2 overexpression inhibits cell migratory and invasive but not OSCC proliferation.

LCN2 expression is either higher or lower in tumour tissues than in relatively normal tissues and reveal pro- or antioncogenic functions because of distinct functions of LCN2 in different cancer cell types (8). Regarding the pro-oncogenic function, LCN2 is required for Bcr-Abl-induced tumorigenesis in leukaemia cells (29), promoting breast tumour growth (10,14,30) and increasing colon and prostate cancer invasion (12,31).

Pro-oncogenic functions of LCN2 are majorly regulated the promotion of the MMP-9 activity and downregulation of E-cadherin (12–14,31). In contrast to prooncogenic effects, a recent study reported significantly lower LCN2 expression in metastatic tissues than in primary tumours of several tumour types (8), which is similar to our findings in OSCC. LCN2 has been reported to suppress the in vitro proliferation or invasion and *in vivo* tumour growth or metastasis of several tumours, such as those of the liver (32), breast (33), colon (34) and pancreatic (35) cancers. The present study is consistent with previous reports that state that LCN2 overexpression in OSCC cells suppress *in vitro* cell migration, invasion and *in vivo* tumour growth and lymph node metastasis. Presently, the mechanisms underlying the LCN2-induced suppression of tumour metastasis are not well defined. This study first revealed that LCN2 inhibited OSCC cell invasion and metastasis, possibly by suppressing HIF-1α-mediated CAIX expression. CAIX, a transmembrane zinc metalloenzyme, is overexpressed in different human cancers and is crucial in tumour metastasis, including that of OSCC (26,36). CAIX regulates the migration of OSCC cells and correlates with the poor prognosis of patients with OSCC (26). Furthermore, CAIX can be upregulated in OSCC cells after hypoxic exposure and further promoted the invasive ability of cancer cells (37). Thus, HIF-1α-CAIX signalling pathways may be vital in mediating the effects of LCN2 on OSCC invasion. In addition to the transcriptional regulation of CAIX by LCN2 via the HIF-1α pathway, other CA isoenzyme, CAII, is also reported to be post-transcriptionally regulated by microRNAs (miRs), such as miR-23b (38). By combining data from our miRNA screening profiles and miRNA target databases, we first found that LCN2 overexpression in OSCC cells upregulate miR-4505, revealing the suppressive effects on CAIX and cell motility. Several miRNAs, such as miR-210, –155, –10b, –20b and –200b, are upregulated or downregulated in response to hypoxia (39). However, whether the miR-4505 exhibits a hypoxic signature in OSCC should be further investigated in the future.

In addition to the LCN2-regulated CAIX downregulation in OSCC, there exists several possible mechanisms underlying the LCN2-induced suppression of tumour metastasis. In pancreatic cancer, LCN2 partly reduces invasion by suppressing FAK activation (35). The FAK-Src signalling has been reported to regulate cell motility by controlling actin cytoskeletal rearrangement (40,41). In this study, we observed that LCN2 overexpression in OSCC cells suppressed FAK activation and the subsequent Src phosphorylation (Supplementary Figure 6B, available at *Carcinogenesis* Online). Moreover, LCN2-overexpressing cells revealed few F-actin-containing microfilament bundles compared with control cells (Supplementary Figure 6A, available at *Carcinogenesis* Online). Future studies will address the mechanism by which LCN2 regulates FAK activation in OSCC.

The inhibition of EMT is another mechanism underlying LCN2-induced suppression of tumour metastasis. In our study, we observed that LCN2 overexpression in SCC9 cells increased the expression of E-cadherin (Supplementary Figure 6C, available at *Carcinogenesis* Online). Wang *et al.* (32) reported that LCN2 can inhibit EMT by suppressing the transcriptional repressor of E-cadherin, Twist1, in liver cancer. Actually, Twist has been reported to be a direct downstream target of HIF-1α to promote metastasis of head and neck cancer (42). We suggested that LCN2 inhibited OSCC cell metastasis, also possibly by suppressing HIF-1α-mediated Twist expression. In addition to HIF-1α Twist signalling pathway, LCN2 can restore E-cadherin expression by affecting the Ras-MAPK pathway in Ras-transformed mammary tumour cells (33). Moreover, FAK-Src signalling has been reported to involve in TGF-β-induced EMT (43). Thus, an additional study is required for delineating the interactions between Ras-MAPK signalling or FAK-Src signalling and LCN2-mediated E-cadherin upregulation in OSCC cells.

To our knowledge, this study is the first to report the clinical and prognostic significance of LCN2 in OSCC among the Taiwanese population. Moreover, we observed that LCN2 suppresses cell motility by downregulating CAIX protein level via HIF-1α-mediated transcriptional regulation and miR-4505-mediated post-transcriptional regulation. These findings provide new insight into the role of LCN2 and its molecular mechanism in OSCC progression, suggesting LCN2 as a potential diagnostic and therapeutic target in oral cancer.

Supplementary material

Supplementary Tables 1–4 and Figures 1–6 can be found at http://carcin.oxfordjournals.org/

Funding

This study was supported by a grant from Wan Fang Hospital-Taipei Medical University (105 swf07). This study was also supported by Grant CSH-2014-C-020 from Chung Shan Medical University Hospital, Taiwan. The funders had no role in the study design, data collection and analysis, decision to publish or manuscript preparation.

Conflict of Interest Statement: None declared.

References

1. Bagan, J.V. et al. (2008) Recent advances in Oral Oncology 2007: epidemiology, aetiopathogenesis, diagnosis and prognostication. Oral Oncol., 44, 103–108.
2. Forastiere, A. et al. (2001) Head and neck cancer. N. Engl. J. Med., 345, 1890–1900.
3. Gil, Z. et al. (2009) Lymph node density is a significant predictor of outcome in patients with oral cancer. Cancer, 115, 5700–5710.
4. Mamelle, G. et al. (1994) Lymph node prognostic factors in head and neck squamous cell carcinomas. Am. J. Surg., 168, 494–498.
5. Flower, D.R. (1996) The lipocalin protein family: structure and function. Biochem. J., 318, 1–14.
6. Goetz, D.H. et al. (2002) The neutrophil lipocalin NGAL is a bacteriostatic agent that interferes with siderophore-mediated iron acquisition. Mol. Cell, 10, 1033–1043.
7. Catalán, V. et al. (2009) Increased adipose tissue expression of lipocalin-2 in obesity is related to inflammation and matrix metalloproteinase-2 and metalloproteinase-9 activities in humans. J. Mol. Med. (Berl)., 87, 803–813.
8. Candido, S. et al. (2014) Roles of neutrophil gelatinase-associated lipocalin (NGAL) in human cancer. Oncotarget, 5, 1576–1594.
9. Yang, J. et al. (2009) Lipocalin 2: a multifaceted modulator of human cancer. Cell Cycle, 8, 2347–2352.
10. Yang, J. et al. (2009) Lipocalin 2 promotes breast cancer progression. Proc. Natl. Acad. Sci. USA, 106, 3913–3918.
11. Berger, T. et al. (2010) Disruption of the Lcn2 gene in mice suppresses primary mammary tumor formation but does not decrease lung metastasis. Proc. Natl. Acad. Sci. USA, 107, 2995–3000.
12. Ding, G. et al. (2015) Over-expression of lipocalin 2 promotes cell migration and invasion through activating ERK signaling to increase SLUG expression in prostate cancer. Prostate, 75, 957–968.
13. Yan, L. et al. (2001) The high molecular weight urinary matrix metalloproteinase (MMP) activity is a complex of gelatinase B/MMP-9 and neutrophil gelatinase-associated lipocalin (NGAL). Modulation of MMP-9 activity by NGAL. J. Biol. Chem., 276, 37258–37265.
14. Fernández, C.A. et al. (2005) The matrix metalloproteinase-9/neutrophil gelatinase-associated lipocalin complex plays a role in breast

tumor growth and is present in the urine of breast cancer patients. Clin. Cancer Res., 11, 5390–5395.
15. Kubben, F.J. et al. (2007) Clinical evidence for a protective role of lipocalin-2 against MMP-9 autodegradation and the impact for gastric cancer. Eur. J. Cancer, 43, 1869–1876.
16. Lim, R. et al. (2007) Neutrophil gelatinase-associated lipocalin (NGAL) an early-screening biomarker for ovarian cancer: NGAL is associated with epidermal growth factor-induced epithelio-mesenchymal transition. Int. J. Cancer, 120, 2426–2434.
17. Warnakulasuriya, S. (2009) Global epidemiology of oral and oropharyngeal cancer. Oral Oncol., 45, 309–316.
18. Lin, S.H. et al. (2014) Casein kinase 1 epsilon expression predicts poorer prognosis in low T-stage oral cancer patients. Int. J. Mol. Sci., 15, 2876–2891.
19. Chien, M.H. et al. (2012) Tumor-associated carbonic anhydrase XII is linked to the growth of primary oral squamous cell carcinoma and its poor prognosis. Oral Oncol., 48, 417–423.
20. Kok, S.H. et al. (2007) Establishment and characterization of a tumorigenic cell line from areca quid and tobacco smoke-associated buccal carcinoma. Oral Oncol., 43, 639–647.
21. Yang, C.Y. et al. (1994) Regulation of PG synthase by EGF and PDGF in human oral, breast, stomach, and fibrosarcoma cancer cell lines. J. Dent. Res., 73, 1407–1415.
22. Yang, S.F. et al. (2015) Upregulation of miR-328 and inhibition of CREB-DNA-binding activity are critical for resveratrol-mediated suppression of matrix metalloproteinase-2 and subsequent metastatic ability in human osteosarcomas. Oncotarget, 6, 2736–2753.
23. Yang, S.F. et al. (2010) Antimetastatic effects of *Terminalia catappa* L. on oral cancer via a down-regulation of metastasis-associated proteases. Food Chem. Toxicol., 48, 1052–1058.
24. Chien, M.H. et al. (2015) Keap1-Nrf2 interaction suppresses cell motility in lung adenocarcinomas by targeting the S100P protein. Clin. Cancer Res., 21, 4719–4732.
25. Pastorekova, S. et al. (2008) Cancer-associated carbonic anhydrases and their inhibition. Curr. Pharm. Des., 14, 685–698.
26. Yang, J.S. et al. (2015) Carbonic anhydrase IX overexpression regulates the migration and progression in oral squamous cell carcinoma. Tumour Biol., 36, 9517–9524.
27. Kong, D. et al. (2015) miR-1271 inhibits OSCC cell growth and metastasis by targeting ALK. Neoplasma, 62, 559–566.
28. Lea, J. et al. (2010) Metastases to level IIb in squamous cell carcinoma of the oral cavity: a systematic review and meta-analysis. Head Neck, 32, 184–190.
29. Leng, X. et al. (2008) Lipocalin 2 is required for BCR-ABL-induced tumorigenesis. Oncogene, 27, 6110–6119.
30. Leng, X. et al. (2009) Inhibition of lipocalin 2 impairs breast tumorigenesis and metastasis. Cancer Res., 69, 8579–8584.
31. Hu, L. et al. (2009) NGAL decreases E-cadherin-mediated cell-cell adhesion and increases cell motility and invasion through Rac1 in colon carcinoma cells. Lab. Invest., 89, 531–548.
32. Wang, Y.P. et al. (2013) Lipocalin-2 negatively modulates the epithelial-to-mesenchymal transition in hepatocellular carcinoma through the epidermal growth factor (TGF-beta1)/Lcn2/Twist1 pathway. Hepatology, 58, 1349–1361.
33. Hanai, J. et al. (2005) Lipocalin 2 diminishes invasiveness and metastasis of Ras-transformed cells. J. Biol. Chem., 280, 13641–13647.
34. Lee, H.J. et al. (2006) Ectopic expression of neutrophil gelatinase-associated lipocalin suppresses the invasion and liver metastasis of colon cancer cells. Int. J. Cancer, 118, 2490–2497.
35. Tong, Z. et al. (2008) Neutrophil gelatinase-associated lipocalin: a novel suppressor of invasion and angiogenesis in pancreatic cancer. Cancer Res., 68, 6100–6108.
36. Shin, H.J. et al. (2011) Carbonic anhydrase IX (CA9) modulates tumor-associated cell migration and invasion. J. Cell Sci., 124, 1077–1087.
37. Teppo, S. et al. (2013) The hypoxic tumor microenvironment regulates invasion of aggressive oral carcinoma cells. Exp. Cell Res., 319, 376–389.
38. Torella, D. et al. (2014) Carbonic anhydrase activation is associated with worsened pathological remodeling in human ischemic diabetic cardiomyopathy. J. Am. Heart Assoc., 3, e000434.
39. Shen, G. et al. (2013) Hypoxia-regulated microRNAs in human cancer. Acta Pharmacol. Sin., 34, 336–341.
40. Wei, H. et al. (2011) Abnormal cell properties and down-regulated FAK-Src complex signaling in B lymphoblasts of autistic subjects. Am. J. Pathol., 179, 66–74.
41. Hsia, D.A. et al. (2003) Differential regulation of cell motility and invasion by FAK. J. Cell Biol., 160, 753–767.
42. Yang, M.H. et al. (2008) Direct regulation of TWIST by HIF-1alpha promotes metastasis. Nat. Cell Biol., 10, 295–305.
43. Cicchini, C. et al. (2008) TGFbeta-induced EMT requires focal adhesion kinase (FAK) signaling. Exp. Cell Res., 314, 143–152.